J. C. Trinder
*School of Surveying*
*University of New South Wales*
*Kensington, N.S.W. 2033, Australia*

# Pointing Precisions on Aerial Photography

Pointing precisions of test targets on both artificial and real aerial photographs reveal that precisions of 1 μm or better are attainable under conditions of high image quality and high optical magnification.

Abstract: *In previous research visual pointing observations on noisy sharp objects were investigated as a first stage in determining the characteristics of visual observations to photographic images. This paper will describe laboratory investigations of blurred noisy images which may occur in practice; from these observations estimates of the relationship between image quality combined with viewing optical magnification, and pointing precisions will be made. To relate these estimates to practice, 13 aerial photographic missions have been flown. Image quality of the photography was determined and visual observations were made on ground targets. There was good agreement between measurements made on the photography and those derived in the laboratory. Pointing precisions of targets on color photography were superior to those on black-and-white photography for small circular targets and cross-type targets.*

## Introduction

The lack of sharpness, or blur, in photographic images is caused by the inability of optical and photographic elements of the photographic system to reproduce the exact luminance intensity characteristics of the object onto the image medium. In Trinder (1971) the properties of the image of blurred targets which proved to be significant in determining pointing precision were the size of *annulus* between the edge of the measuring mark (MM) and the target, and the *slope of the density profile* of the target. Noise in the image was expressed in terms of a *signal-to-noise ratio* (SNR) in Trinder (1982) for studying the effects of noise on sharp targets on pointing, detection, and recognition observations. To relate the slope of the density profile to characteristics of imaging systems, either experimental laboratory tests or theoretical computations must be carried out based on specific image quality and target characteristics. Because the point spread functions (PSF) of photographic systems closely approximate Gaussian PSF's, convolutions of Gaussian PSF's and circular and cross-type targets (Trinder, 1973, 1974) were computed in order to determine the slopes of the density profiles for a wide range of PSF and target sizes. The slope of the density profile has been adopted as the parameter of blur for the observations on blurred noisy targets described in this paper. This slope has been related to Gaussian spread functions and modulation transfer functions (MTF's) using the results of the earlier computations (Trinder, 1973).

## Laboratory Investigations

### Observations

Blurred noisy targets required for the observations were produced by a similar photographic process to that used by Trinder (1982) to produce sharp noisy targets, the blur being created by modifying the settings of the printing camera such that the images of the targets were slightly out of focus. Target sizes ranged from 2.9 mrad (annulus width of 0.7 mrad or 29 μm at 6× optical magnification) to 13.5 mrad (annulus width of 6.2 mrad or 250 μm at 6× optical magnification), shown typically in Figure 1.

A complex photographic procedure was required to obtain satisfactory levels of both blur and noise. Noise is defined (Trinder, 1982) in terms of root-mean-square (RMS) granularity determined by scan-

Photogrammetric Engineering and Remote Sensing,
Vol. 50, No. 10, October 1984, pp. 1449-1462.

0099-1112/84/5010-1449$02.25/0

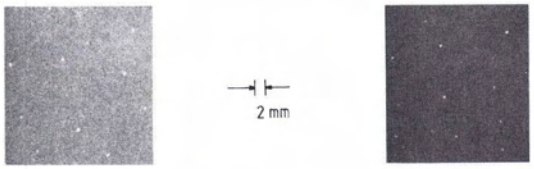


FIG. 1. Typical blurred noisy targets used for laboratory observations.

ning a sample with a circular aperture diameter equivalent to 48 μm when the viewing magnification is 12×, the RMS granularity being inversely proportional to the aperture diameter. Because the viewing aperture of the eye is inversely proportional to the optical magnification, an aperture of 96 μm was used for this study because the optical magnification of the stereoplotter was 6×. The SNR of an isolated target is defined as the ratio of the density difference above background and the RMS granularity.

Slopes of the density profiles of the blurred targets were determined by measurement with a small circular aperture on a set of identical targets printed without superimposed noise. This estimate of quality does not include the quality of the stereoplotter optics, though the pointing precisions derived are subject to the quality of the optics. Assuming that the optics of most stereoplotters are similar, this study is representative. Monocular pointing precisions were derived on a Wild A8 stereoplotter with a measuring mark of 60 μm, as in Trinder (1982), and all measurements were converted to angular subtense using the formula

$$\text{angular subtense (mrad)} = \frac{\text{linear distance (μm)} \times \text{optical magnification}}{250} \quad (1)$$

where 250 mm is the observation distance for comfortable viewing. Seven sets of 15 monocular observations were made on about 110 visible targets of different sizes subject to varying degrees of noise and blur; a pooled standard deviation was determined, following statistical tests on the seven sets of observations. Typical results of these observations are given in Figure 2 expressed in terms of SNR, with the target blur and the slope of the density profile (in $\Delta D$/mrad) shown for each plotted position. As occurred with the observations to noisy targets, there were significant variations in the distribution of the precisions of observations, which were apparently caused by the statistical distribution of the noise components in the images. Figure 2 has been derived from three target annulus sizes of 167 μm, 213 μm, and 258 μm (target sizes of 9.5, 11.6, and 13.5 mrad, respectively), pointing precisions for 167 μm and 258 μm being scaled linearly to determine the equivalent value for an annulus of 213 μm. This step is justified because O'Connor (1967) and Trinder (1971) have shown that the most significant parameter of a target affecting pointing precisions is the target annulus width, and that there is a linear relationship between annulus width and pointing precisions for annulus widths greater than about 2 mrad. In Trinder (1971) it was shown that there is no correlation between the parameters of annulus

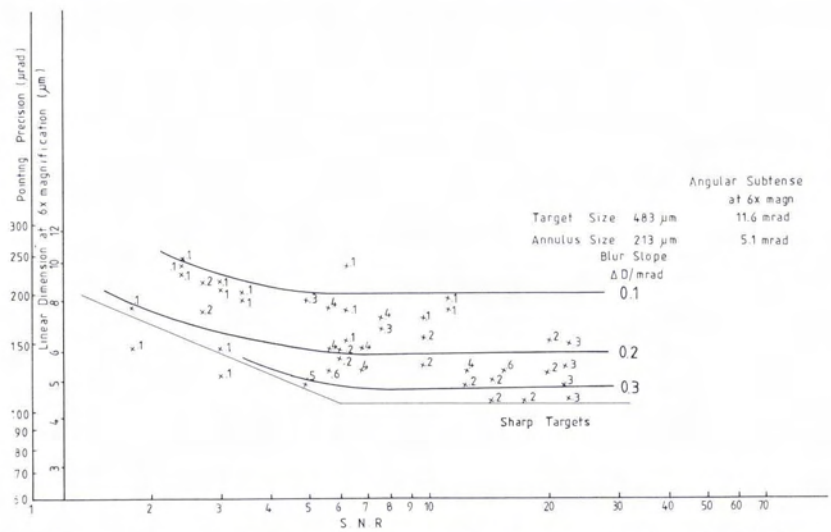


FIG. 2. Pointing precisions for blurred noisy targets 483 μm in diameter viewed at 6× magnification (annulus = 213 μm) expressed in terms of SNR. The slope of the density profile of each target is shown against the plotted position. Observer is PY.

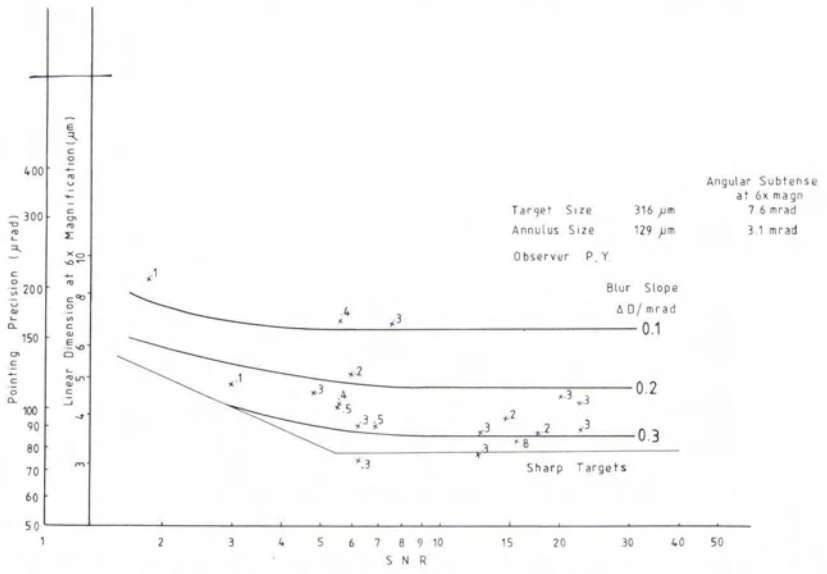


FIG. 3. Pointing precisions for blurred noisy targets 316 μm in diameter viewed at 6× magnification (annulus = 129 μm) expressed in terms of SNR. The slope of the density profile of each target is shown against the plotted position. Observer is PY.

width and target blur. It may therefore be reasonably assumed that there is no correlation between the width of the annulus and either blur or SNR. However, there is correlation between the latter two factors. This is confirmed by the fact that the patterns of visual performance for targets subject separately to blur and noise are almost identical. Such correlation was also indicated in interpretation experiments by Snyder *et al.* (1982).

Figures 3 and 4 have been derived from observations of two separate observers, PY and KB, for target annulus sizes of 129 μm based on results for targets with annulus sizes of 96 μm and 129 μm (Target sizes of 5.9 mrad and 7.6 mrad). A further figure was derived for an annulus size of 30 μm (Target size of 2.9 mrad), but is not presented because of its similarity to Figures 3 and 4.

## DISCUSSION OF RESULTS FOR BLURRED NOISY TARGETS

From Trinder (1971) it is known that, for slopes below a certain value which is dependent on target annulus size, pointing precisions deteriorate as the slope of the density profile decreases. The magnitudes of pointing precisions in Figures 2, 3, and 4 are not the same as those in Trinder (1971), which were derived by two different observers under different observation conditions on a precise mea-

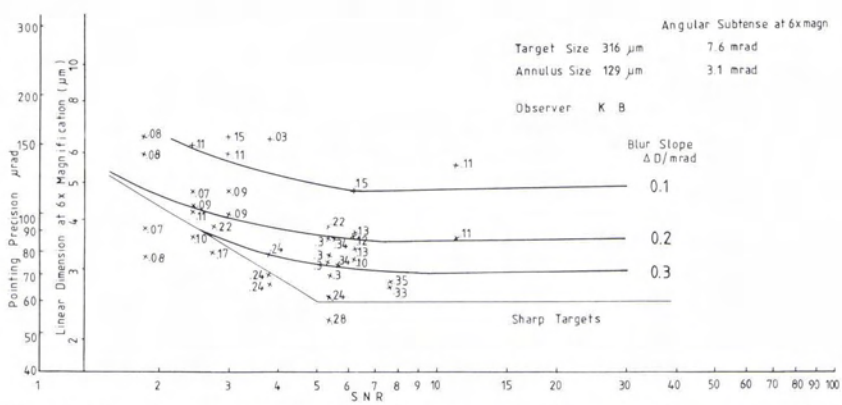


FIG. 4. Pointing precisions for blurred noisy targets 316 μm in diameter viewed at 6× magnification (annulus = 129μm) expressed in terms of SNR. The slope of the density profile of each target is shown against the plotted position. Observer is KB.

suring system with no optical components between the target and the observer. Interpolated curves in Figures 2, 3, and 4 have been determined incorporating known relationships in Trinder (1971) with regard to blur and in Trinder (1982) with regard to effects of noise

At high SNR's the pointing precisions deteriorate as blur increases, but as SNR's decrease the blur and noise interact and, hence, are correlated. At low SNR's, the pointing precisions become less dependent on blur and more on noise. These findings differ from those of Snyder *et al.* (1982), who claim that noise had little effect on a very blurred target, but that blur did affect observations on very noisy targets. They also claim that, for interpretation tasks, observers react differently to these two effects. For pointing observations, the interaction between the effects of blur and noise depends on the magnitude of each. The threshold value of SNR below which pointing precisions are affected is about 5 or 6 while the threshold level of blur is about 0.4 $\Delta D$/mrad. It is only below these values that interaction can be considered. The optical magnifications used by the observers of Snyder *et al.* (1982) are not available, and therefore direct comparisons with their study are impossible.

The combined effects of blur and noise have been presented in Figure 5 from observations derived in this paper for observer PY. As demonstrated by Trinder (1971, 1982), the lines relating pointing precision to target size and constant image quality move up the graph, but remain parallel to the line for sharp noiseless targets as image quality deteriorates. The numbered lines in Figure 5 have been derived from particular combinations of target blur and SNR, as shown in the attached nomogram. To reference Figure 5, parameters of the blur and SNR of the target must be obtained and input to the nomogram to find the specific line applicable.

- Blur can be derived from the measurement of the density profile of the target on a microdensitometer. Alternatively, it can be derived theoretically by computation if the spread function or MTF of the photogrammetric system are known. This proce-

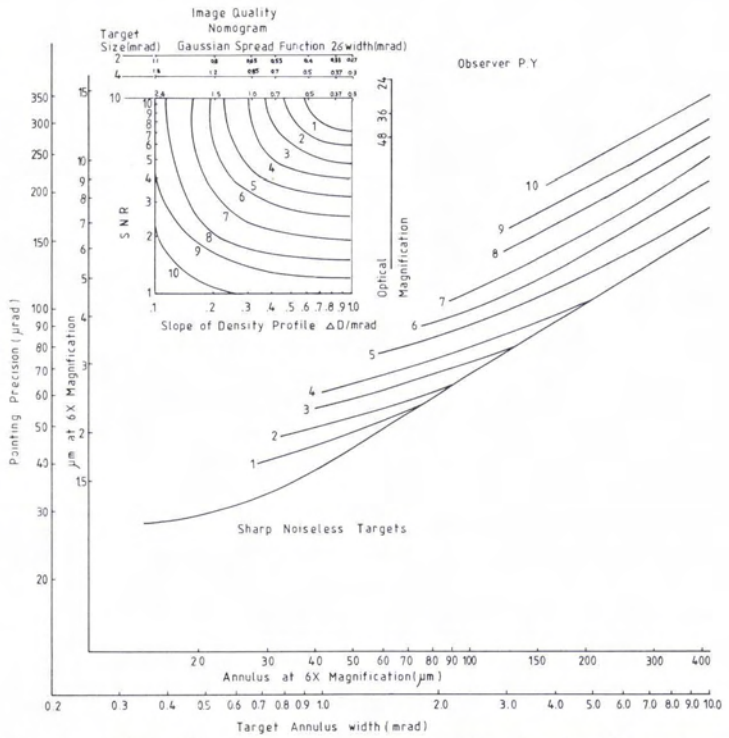


FIG. 5. Relationship between pointing precisions (μrad) and target annulus size (mrad) for circular targets subject to different levels of blur and noise. Dimensions at 6× optical magnification have been added to each axis. The numbered lines must be referenced by inserting target blue ($\Delta D$/mrad) and SNR in the nomogram. For a specific example of target contrast of 5:1 (density difference = 0.7), the typical Guassian spread function 2σ-widths (mrad) which would cause the density slopes for three target sizes are shown at the top of the nomogram. Likewise, the optical magnifications corresponding with the SNR's for an RMS granularity of 0.03$D$ for a scanning aperture of 48 μm and target contrasts of 5:1 are shown to the right of the nomogram.

dure was adopted in the computations presented by Trinder (1973), in which Gaussian spread functions were assumed. Typical Gaussian spread function widths derived for three target sizes of contrast 5:1 are shown on the top of the nomogram. Equation 1 should be used to convert angular measurement to linear dimensions at a specific optical magnification. This expression of image quality is based on the optics of the stereoplotter being similar to that of the Wild A8. If the quality of the optics is either better or worse than the Wild A8, some modification of the use of the nomogram will be necessary.

- SNR must be derived from the measurements of target density above background and the RMS granularity of the film emulsion used for the photography. The scanning diameter of granularity must be appropriate to the optical magnification to be used for the observations. If scanning for RMS granularity is not possible, representative values are available in manufacturers' handbooks, while detailed measurements for a number of film and developer combinations are given in Trinder (1980). Optical magnifications which correspond to the SNR's for a target contrast of 5:1 and RMS granularity of 0.03D measured with an aperture of 48 μm, are shown to the right of the nomogram.

Investigations given in Trinder (1982) and in this paper have been based on several observers, each one having his/her own personal characteristics. Figure 5 has been derived from the observations of PY to maintain consistency, while the earlier observations in Trinder (1982) were obtained primarily by observer KB. Observations made on the aerial photography presented later in this paper were made by PY and EW. Each of these observers was trained on a standard sharp target calibration set, differences between them amounting to about 25 percent. However, in all cases behaviour trends remained consistent with those presented in this paper; therefore, the pattern of results in Figure 5 is applicable to practical situations. The application of these results to measurements in practice can be used to determine relative changes in pointing precisions as a function of image quality parameters and a good estimate of absolute pointing precisions. The exact absolute values of pointing precisions, however, are dependent on particular observer characteristics, which must be determined by extensive investigations of that observer. The results of 6× optical magnification have been extrapolated to 36× magnification later in this paper because the visual system performs according to the angular subtense of an object. No measuring system was available for measurements to precisions better than 1 μm; therefore, observations at such high magnifications have not been made. These predictions, however, are confidently made on the basis of known characteristics of the visual system.

### SPATIAL FREQUENCY DOMAIN

In Trinder (1982) the power spectra of seven targets and the Wiener spectrum of noise were computed to determine the relationship between pointing precisions and characteristics of these spectra. Further computations have been made on the power spectra of blurred targets, the blur being introduced as Gaussian spread functions described by the $2\sigma$-width of the curve. The spread function widths for which the density slope is approximately 0.4 $\Delta D$/mrad for two target contrasts are shown in Figure 6. The computations reveal that the power spectra shapes, characterized by the maxima and frequency ranges, are only marginally affected for small levels of blur, depending on target contrast, but the maxima and frequency ranges of the targets are both affected as the blur increases.

It is clear that the deterioration in pointing pre-

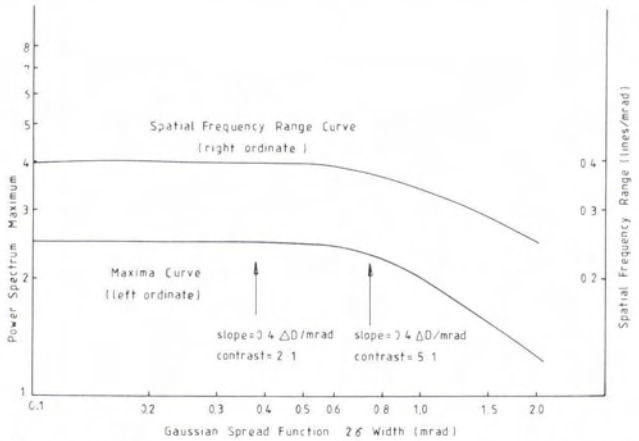


FIG. 6. Power spectra maxima and frequency range for a target of 5.9 mrad subject to Gaussian spread function blur as shown. The points at which the slope of the density profile is 0.4 ΔD/mrad for a target contrast of 2:1 and 5:1 are shown.

cision with increased blur is related to the shapes of the power spectra. In Trinder (1982), it was claimed that the maxima of the power spectra contribute to the target visibility, and the spatial frequency range, to the apparent sharpness. The maximum for a particular target size will change according to the contrast of the object; therefore, it is not the primary factor affecting pointing precision, provided the contrast is well above threshold. Spatial frequency range, therefore, is the factor which has the primary effect on the ability to measure to targets, because target contrast does not affect the frequency range. In Trinder (1982) it was shown that noise can also contribute to the reduction in frequency range and, hence, pointing precision.

Hufnagel (1965) has shown that MTFA, the area between the MTF curve of an optical system and the contrast threshold of an observer's visual system, can be related to visual performance. In this paper, the area under the spatial frequency curve of the targets is clearly related to visual performance. However, even though the most significant parameter is the spatial frequency range, it is not the only factor, because the frequency range of targets with the same pointing precision but different sizes is not the same. For example, the pointing precisions of a sharp target 13.9 mrad (annulus 6.2 mrad) and a 5.9 mrad blurred target (2.2 mrad annulus) with slope of 0.17 $\Delta D$/mrad are the same, but the spatial frequency ranges are not. There is, therefore, no simple relationship between the power spectra and visual performance.

### DETECTION AND RECOGNITION

The tasks of detection and recognition of geometric shapes of circle, diamond, triangle, and square were investigated for noisy targets in Trinder (1982) and studied in this paper for blurred noisy targets. Due to a change in observer, this section of the work could not be investigated thoroughly. The 75 percent probability of detection and recognition of blurred noisy targets is shown in Figure 7, revealing that the relationship between SNR and target size for constant target profile slope moves higher on the graph as the image quality deteriorates. Both detection and recognition deteriorate rapidly as image quality decreases. The significance of these results is that relationships between visual tasks of pointing and recognition and parameters of image quality can be formulated in a similar manner.

### PRACTICAL APPLICATIONS

To demonstrate the relationship between target image quality characteristics, optical magnification, and pointing presicions, three target sizes of 118 μm, 148 μm, and 177 μm have been selected while the measuring mark of the observation instrument is 60 μm. Optical magnifications are assumed to vary from 6×, 12×, 24×, and 36×. RMS granularity is 0.03$D$ at gross density of 1.0 for a scanning aperture of 48 μm, which is typical of aerial photographic materials printed with a gamma of about 1.2. Image quality is defined by Gaussian spread function 2σ-widths of 10 μm, 20 μm, and 30 μm, which closely approximate the image quality of aerial photographic systems. It is assumed that the quality of the optics in the stereoplotter used for the measurements would be similar to that of the Wild A8 optics. The equivalent MTF's derived from the Gaussian point spread functions exp $(-x^2/2\sigma^2)$ are given by the normalization of the expression $2\pi\sigma^2$ exp $(-2\pi^2\omega^2)$, where ω is the spatial frequency, and are shown in Figure 8.

Target contrasts of 2:1 ($\Delta D$ = 0.3) and 5:1 ($\Delta D$ =

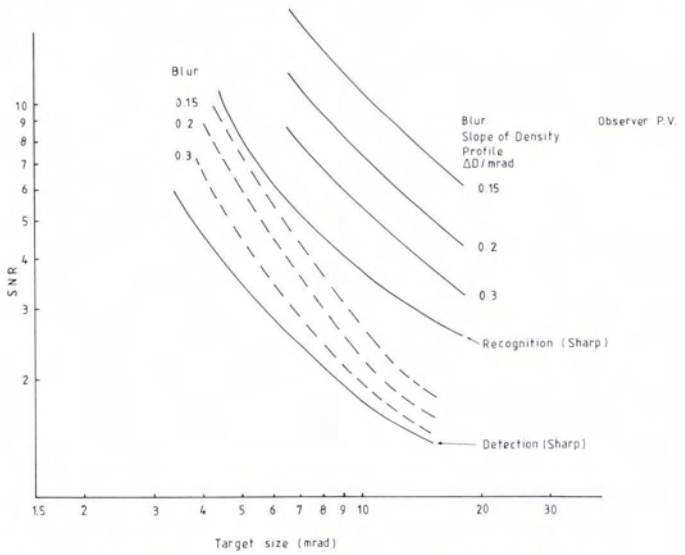


FIG. 7. Relationship between target size, SNR, and target blur for the tasks of recognition and detection for the four target shapes studied.

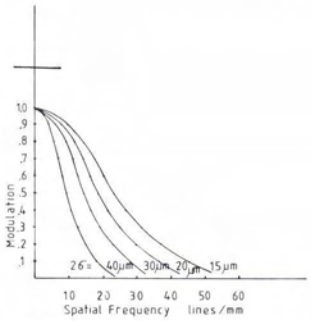


FIG. 8. MTF's derived from Gaussian spread functions with 2σ-widths as shown.

0.7) have also been assumed, giving SNR's ranging from 20 and 47, respectively, for 6× optical magnification, and 3 and 8 for 36× optical magnification. For these variables, Figures 9 and 10 have been drawn for target contrasts of 2:1 and 5:1, respectively. The optimum optical magnification is dependent on the image quality of the photography; the lower the image quality, the lower the optimum magnification and, logically, the pointing precision. A similar statement may be made also with respect to target contrast, because it affects the target density profile.

Pointing precisions of 1μm or better are potentially attainable by an observer using a suffficiently precise measuring instrument, provided the conditions of high contrast and high image quality, including that of the stereoplotter, exist. Under such circumstances granularity of normal aerial photographic materials would only affect precisions for optical magnifications 36× or greater, which is also revealed in Figure 5. Granularity will have an increasing effect on precisions as contrast decreases, or indeed if RMS granularity is larger. However, even if RMS granularity is doubled, the effect on pointing precisions at high magnifications is marginal. It is probable that the quality of the stereoplotter optics would have to be better than that available in the Wild A8 or similar stereoplotters if very high optical magnification were to be used. However, no comparative measurements of plotter optics have been made. For standard aerial photographic missions for which the 2σ-width of the spread function would typically range from 15 μm to 30 μm, pointing precisions of 1.5 μm to 2 μm can be achieved.

The choice of optimum target sizes for each optical mangification and spread function width are summarized for a measuring mark size of 60 μm in Table 1, which displays a comprehensive range of values suitable for all practical cases. For other measuring mark sizes, it is sufficient to adjust the given target sizes in Table 1 by the formula (MM chosen − 60 μm)/2.

The fact that the optimum target sizes are dependent on magnification is important. If, for example, a target size of 120 μm, suitable for 6× magnification, were viewed at 24× magnification, a pointing precision of 1.7 μm would be obtained because the annulus is too large. This is an increase of 30 percent and may be significant if the highest accuracy is being sought.

However, more significantly, if the 100 μm target selected for 24× optical magnification were measured at 6× optical magnification with a 60 μm measuring mark, the pointing precision on the smaller annulus target may remain the same as for the optimum size, but the pointing presicion may deteriorate rapidly if the image quality is not high. The measuring precisions of points on photography are largely dependent on the selection of the correct size of ground target to suit both optical magnification and measuring mark sizes. Special attention should be given to this selection, for topographic or non-topographic photogrammetric applications.

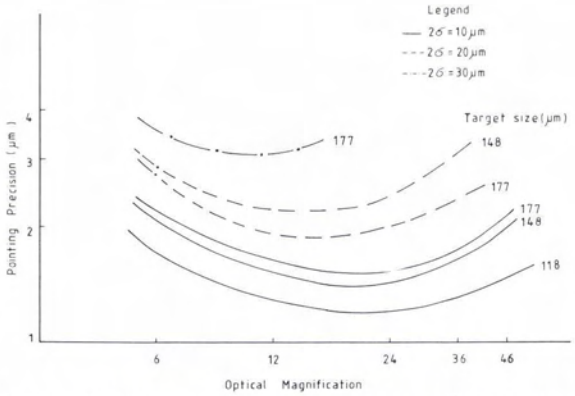


FIG. 9. Relationship between optical magnification and pointing precision for three target sizes subject to three levels of image quality expressed as a Gaussian spread function 2σ-width. The RMS granularity is assumed to be 0.03*D* for a scanning aperture of 48 μm. Target contrast was 2:1.

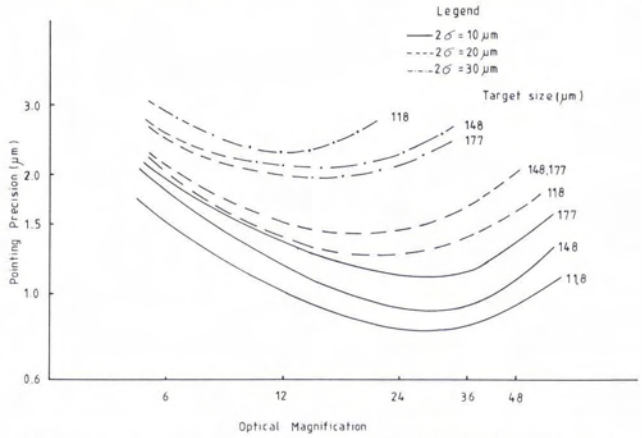


FIG. 10. Relationship between optical magnification and pointing precision for three target sizes subject to three levels of image quality expressed as a Gaussian spread function $2\sigma$-width. The RMS granularity is assumed to be $0.03D$ for a scanning aperture of 48 μm. Target contrast was 5:1.

The possibility of obtaining pointing precisions less than 1 μm if high optical magnifications are used, and the image quality of the photography and the stereoplotter optics are very high, indicates that the visual capabilities of an observer are not the limiting factor in coordinate measurement. Indeed, a precision of 1 μm or better should be aimed for in order to obtain the highest potential from photography. The limiting factors in the measurement of coordinates appear to be the quality of the images currently available, the quality of the optics of stereoplotters which may reduce the inherent photograph quality, and the geometry of the photograph. These components in the measurement chain should be studied and improved if the full potential of photogrammetry is to be utilized.

## AERIAL PHOTOGRAPHY TESTS

### PHOTOGRAPHY MISSIONS

This research program has so far been based almost exclusively on laboratory observations. At the termination of the laboratory stage, aerial photography was requested in order to compare the results derived from the laboratory studies with those obtained under practical conditions. The task required the measurement of image quality and its relationship with pointing precisions.

Twelve black-and-white aerial photography missions were flown with specifications derived from all combinations of two RC10 camera lenses, 88 mm and 150 mm focal lengths, with and without a red filter, and three flying heights, 1200 m, 2420 m, and 6000 m. The airspeed was 130 knots except for the flying height photography of 6000 m, for which the airspeed was 160 knots. Shutter speed for photography using the red filter was 1/300 sec, and 1/600 sec without.

The negative aerial film used was Kodak 2405 developed with a gamma of about 1.2, which would result in an RMS granularity of $0.03D$ for a gross density of $1.0D$ (Trinder, 1980). Five sets of three yellow circular targets with black backgrounds of sizes ranging from 1.25 m to 6.5 m were placed in triangles; an individual target 11 m in diameter and three sets of cross-type targets ranging in size from 3.5 m to 7 m were also placed. The photography was undertaken at the Bathurst Airport (a rural airport about 200 km west of Syndey) because the painted runway markings were required for the determination of the image quality of the photography in the vicinity of the ground targets, as shown in Figure 11. These runway markings are 6 m by 30 m in size, painted in white on a bitumen background. Photographs were taken with 90 percent overlap to ensure that the targets were photo-

TABLE 1. OPTIMUM TARGET SIZES AND PRECISIONS (μm)

| Optical Magnification | 6× | | 12× | | 24× | | 36× | |
|---|---|---|---|---|---|---|---|---|
| $2\sigma$-width of spread function | Target Size | Precision | Target Size | Precision | Target Size | Precision | Target Size | Precision |
| 10 μm | 100 | 1.3 | 80 | 0.9 | 80 | 0.7 | 80 | 0.6 |
| 20 μm | 120 | 2.0 | 100 | 1.4 | 100 | 1.3 | 100 | 1.1 |
| 30 μm | 180 | 2.6 | 150 | 2.1 | 140 | 2.0 | — | — |

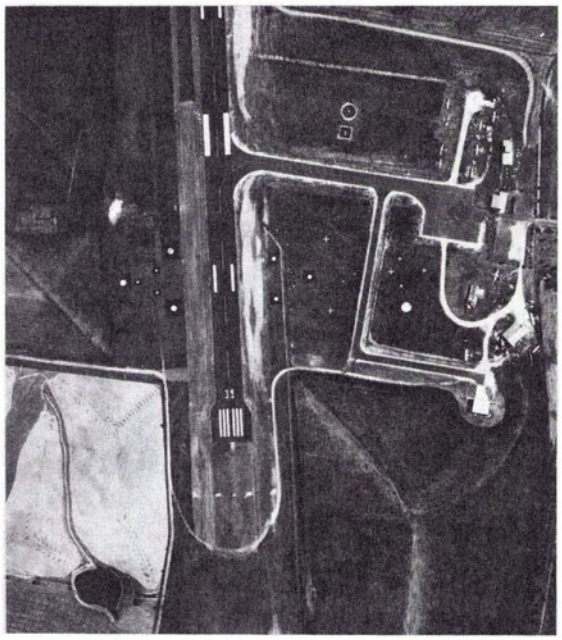


FIG. 11. Test area and targets.

graphed in different positions on the image format. Subsequently, one run of color photography using Kodak color negative film has been taken with the 150-mm lens cone from an elevation of 2130 m. The photographic work was undertaken by the Central Mapping Authority of N.S.W. (CMA) who also laid the targets and surveyed their positions. With such photography a number of aspects of photogrammetry can be studied. Those reported in this paper are

- variation of image quality using different lens cones, and different filters,
- variations in image quality of the negative across the image plane,
- comparison of image quality of positive and negative images,
- relationship between target size and/or quality and pointing precision to confirm laboratory results for circular and cross-type targets, and
- confirmation of results to determine optimum target sizes.

## IMAGE QUALITY OF PHOTOGRAPHY

The image quality of the negative and positive photographs was determined by scanning the airport runway markings with a narrow rectangular slit 1 μm by 150 μm in a Joyce-Loebl microdensitometer, as described by Welch (1971), in the flight direction and at right angles to it for the larger scale photography. Three traces across the markings were derived on at least five positive and negative photographs per run of photography, and a spread function was computed for each trace. A mean spread function was derived for each photograph, and the modulation transfer function (MTF) was computed from the mean. The spread functions closely resembled Gaussian functions in most cases, although there were also examples of asymmetric curves. As the majority of functions were near Gaussian, they have been presented in this study in terms of the $2\sigma$-width measured at the height of 60.6 percent on the spread function curve. The corresponding MTF's computed from the spread functions also closely corresponded to the Fourier Transform of the Gaussian functions in Figure 8.

Spread function widths derived for wide-angle negatives as a function of radial distance are displayed in Figure 12 by separate symbols for along-flight and across-flight directions. MTF's corresponding to three spread function widths are shown to the right of the figure. Odd numbered runs were imaged with the red filter attached, and the even numbers were imaged with an anti-vignetting filter only. While there was significant variation in the plotted results, separation of the data into odd and even numbered runs revealed less variation. Image quality clearly deteriorated towards the edges of the image plane. A summary of the measurements obtained with different camera/filter combinations for negatives is shown in Figure 13. In this figure, the omission of the red filter led to an increase in the size of the spread function, but the deterioration in image quality with radial distance was still evident. There was, indeed, little if any difference in the quality of the photography derived from wide-angle and super wide-angle lenses when the red filter was not used, but the variation in spread function widths derived in these cases was greater than when the red filter was used. The red filter appeared to lead to the production of images which were more reliable and of high quality. There were no significant differences revealed in the image qualities measured in the direction of flight compared with those measured at right angles to the direction of flight.

Attempts to measure the MTF of the positive photographs proved to be more difficult, there being more variation in the measured spread function widths than for the negatives, as revealed in Figure 14. The positive material used was Dupont Cronolar continuous tone film CT-7 with exposure conditions depending on the quality of the negatives. A spread function $2\sigma$-width of the positive material was measured as 18 μm, while RMS granularity was $0.04D$ at gross density of $1.0D$, using a scanning aperture of 48 μm. Convolution of the negative spread functions for the wide-angle photographs with that of the positive material would produce spread function widths varying from about 23 μm to 28 μm, which is within the range of values revealed in Figure 14. The inability to measure positive spread functions appeared to be due mainly to the granularity in the

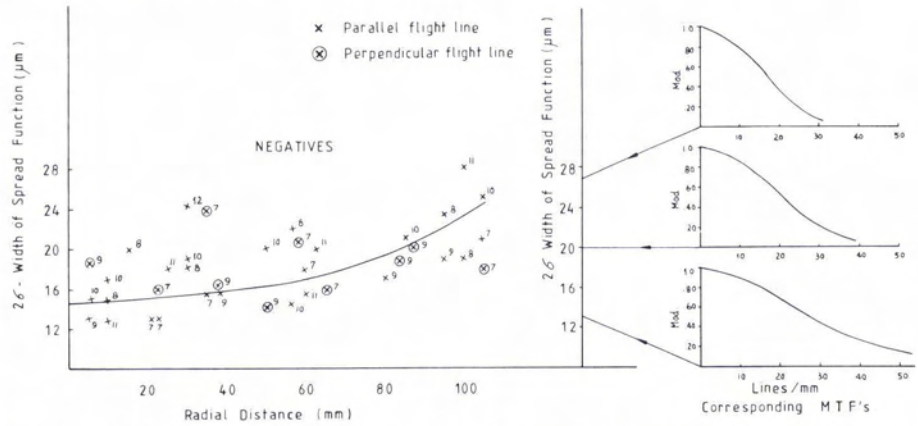


FIG. 12. Spread function 2σ-widths of wide-angle camera in terms of radial distance. MTF's corresponding to three spread functions with 2σ-widths of 13 μm, 20 μm, and 27 μm are also shown. Flying height for runs 7 and 8 is 1200 m; for runs 9 and 10, 2420 m; and for runs 11 and 12, 6000 m.

positive material, which was larger than in the negative.

This study of image quality of the photography reveals that reliable estimates of image quality can be obtained using the techniques described. The accuracies are sufficient to reveal the deterioration in image quality with radial distance from the center of the photograph. In addition, the quality is dependent on the type of filter used, better results being obtained when the red filter was attached.

Spread function shapes were sufficiently reliable to approximate them to Gaussian functions. Consequently, the 2σ-width is a conventient parameter for expressing image quality and has therefore been used as the primary measure of image quality in this section of the study. MTS's, however, are easily determined from the Gaussian spread functions. The spatial frequencies of the MTF's at 0.5 modulation vary from 27 lines/mm for higher quality images to 17 lines/mm, which correspond to spread function 2σ-widths of 13 μm and 27 μm, respectively.

### POINTING PRECISIONS

The second component of this research was the investigation of the precisions of pointing to the targets on the photographs. Circular targets were recommended in Trinder (1974), but crosses (referred to as cross-type) were also studied. Many mapping organizations, including the CMA, use cross-type targets, and this study was designed to compare the suitability of the two types of targets in black-and-white and color. The four smaller circular targets shown in Figure 11 were composed of yellow plastic on a black square background three times the size

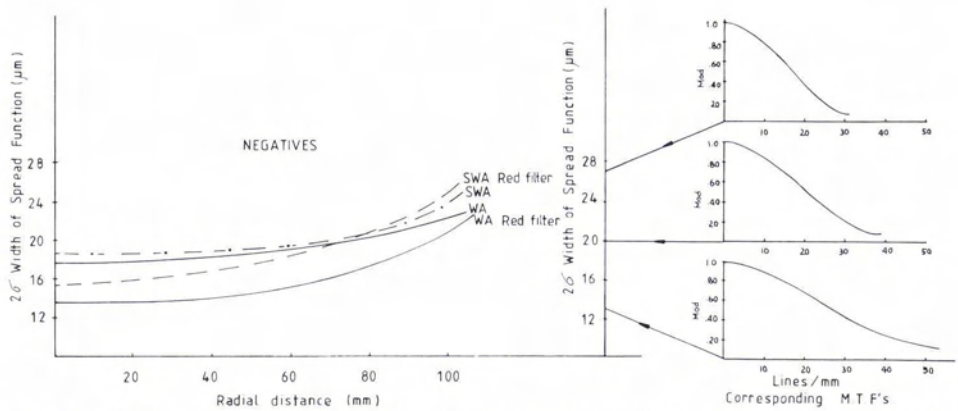


FIG. 13. Summary of spread function 2σ-widths in terms of radial distance derived for camera lens and filter combinations shown. MTF's corresponding to spread functions with 2σ-widths of 13 μm, 20 μm, and 27 μm are also given.

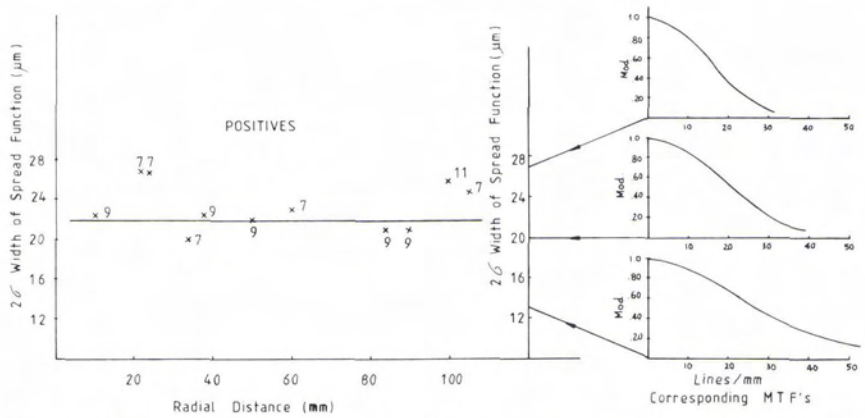


FIG. 14. Spread function 2σ-widths in terms of radial distance for wide-angle camera with the red filter. MTF's corresponding to spread functions with 2σ-widths of 13 μm, 20 μm, and 27 μm are also given.

of the target diameter. The largest target, 11 m in diameter, was placed with a square black surround 13 m square. Cross-type targets were standard sizes used by CMA, being 3.5-m, 4-m, and 7-m square with yellow crosses 0.5-m, 1.0-m, and 1.0-m wide, respectively.

The observation procedure discussed earlier was continued in these investigations. Targets on positives and negatives and color photographs were observed, the photographs being selected such that the targets occurred at different radial distances from the principal point. Results of the observations have been presented in Figures 15 and 16 separately for circular and cross-type targets, based on observations of two observers; each plotted point is the mean of standard deviations obtained in the $x$- and $y$-directions. Both sets of data have been presented in terms of the annulus width between the edge of the target and the measuring mark. In the case of the cross-type targets the annulus was measured to the center of the sides of the square.

## SIGNIFICANT PARAMETERS

*Target Size.* Consistent with results given in Figure 5 for circular artificial targets, the pointing precisions deteriorate with annulus widths above values of about 2 mrad (83 μm at 6× optical magnification). Below 2-mrad annulus widths, pointing

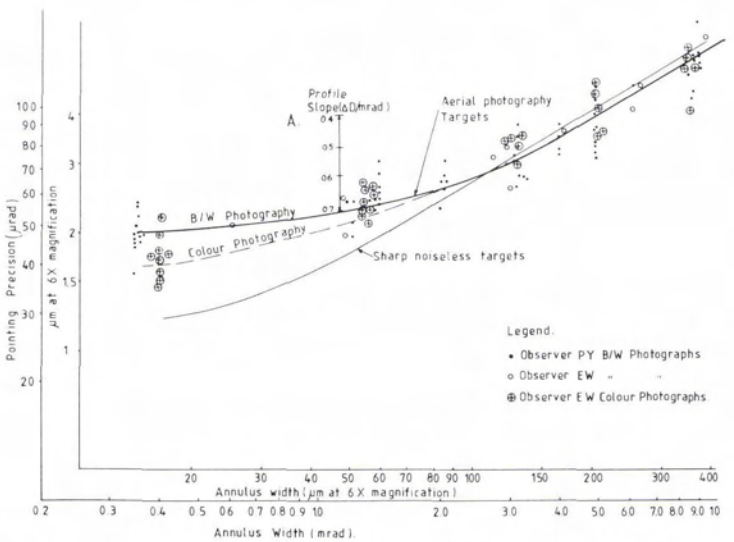


FIG. 15. Pointing precisions derived on circular aerial photography targets expressed in terms of the annulus width between the edge of the target and measuring mark. The line denoted "Sharp noiseless targets" was derived on artificial targets.

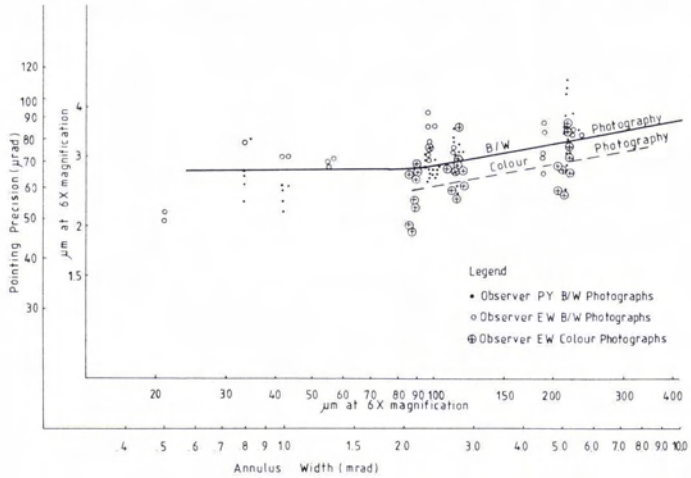


FIG. 16. Pointing precisions derived on cross-type targets expressed in terms of the annulus width between the edge of the target and measuring mark.

precisions become constant, and with further decreases in annulus widths the pointing standard deviations increase. There is no apparent variation between results of positives and negatives even though the positives are of slightly lower image quality. Indeed, the variations in results obtained by each observer are such that differences between pointing precisions for positives and negatives cannot be detected. As described below, the local variations in the image quality of the photographs probably partly contributed to these variations in precisions. The observation of a black measuring mark against a black target on the negative on a white background may also have caused some problems to the observer. Observations on the color photography reveal no unusual trends for the larger targets, but significant improvements for very small annuli. Indeed, the overall precisions for small targets on color photography are 20 percent better than those obtained for black-and-white photography. These pointing precisions approach those possible with black-and-white photography with an image quality equivalent to a Gaussian $2\sigma$-width of 10 μm. If the color photographs are viewed at high magnifications, pointing precisions approaching 1 μm, which it was claimed earlier in this paper should be aimed for, should therefore be possible.

*Image Quality and Granularity.* On the circular targets, the density differences of the targets above background on the black-and-white photography range from 0.4 to 0.7, the majority of targets having a density difference of 0.6. The SNR for the targets at optical magnifications of 6×, therefore, varied from 26 to 47 for the negatives and 20 to 36 for the positives. Such noise levels would not affect pointing precisions. Slopes of the profiles ranged from 0.4 $\Delta D$/mrad to 0.7 $\Delta D$/mrad. In Figure 5 target blur affected pointing observations for slopes of the density profile less than about 0.4 $\Delta D$/mrad, depending on the target size. For targets larger than about 2 to 3 mrad, the effect of blur was less significant. Ziemann (1982) has shown, in extensive observations of calibration photographs, that there is no variation in precision of pointing with respect to radial distance. This result is also confirmed in this study except for the small targets with annuli less than about 1 mrad. The effects of using a stereoplotter with different quality optics will not be significant, unless the new optical system is significantly worse than that of the Wild A8.

To test the effect of target blur, small targets with annuli 1.2 mrad in size located at different radial distances were observed on negative photographs. Blur proved to significantly affect precisions for small targets, as demonstrated in Sections A, Figure 15. The graduations indicate slope of the target profile. In a similar fashion to results in Figures 2, 3, and 4, Section A indicates the possible deterioration in pointing precisions if the slope becomes too small. On the photographs, the slope of the density profile in general deteriorated with increasing radial distance, which is consistent with the results in Figures 12 and 13. However, in some unexpected instances the slope decreased at points towards the center of the photograph. In addition, the slopes in the $x$- and $y$- directions were not always consistent. The quality of the photographic reproduction of localized areas of the negative therefore influenced the pointing precisions. A similar study was not made on the positives because of the expected difficulty in obtaining meaningful slope values.

The cross-type targets were well above the size at which slope would significantly affect the observations. However, similar variations of precisions were also obtained for these targets, as revealed in Figure 15. Cross-type targets reached higher con-

stant levels of precisions than was the case with circular targets, but the rate of deterioration of precisions was less than for the circular targets. For color photography early observations revealed no improvement, but later observations have revealed significant improvements in pointing precisions. The observer required some training period to become accustomed to viewing the colored photographs.

*Choice of Optimum Size of Target.* Optimum target sizes were estimated in laboratory observations (Trinder, 1974). From Figures 15 and 16 the optimum target annulus should be selected at the point where the pointing precision curves become parallel to the abscissa scale. However, the previous discussion indicates that it is wise to estimate target sizes which are too large, rather than too small. For circular targets, therefore, target annulus sizes of 1.3 to 1.5 mrad (54 μm to 63 μm at 6× magnification) would be appropriate, although target annuli as large as 2 mrad (83 μm at 6× magnification) would also be suitable. For cross-type targets, annuli of 2.0 to 2.4 mrad (83 μm to 100 μm at 6× magnification) should be used. These estimates agree well with those made by Trinder (1974), which were 1.35 mrad and 2.2 mrad for circular and cross-type targets, respectively, and those given in Table 1, keeping in mind that the spread function 2σ-width of the photography is 20 to 30 μm.

The optimum target sizes at photograph scale are, therefore, estimated from Figures 15 and 16 for a stereoplotter measuring mark size of 60 μm and an optical magnification of 6×, as 177 μm and 243 μm for circular and cross-type targets, respectively. Pointing precisions resulting are 2.3 μm and 2.5 μm, respectively. These precisions would clearly be reduced if a higher optical magnification were used.

The overall size of cross-type targets recommended in the *Manual of Photogrammetry* (Slama, 1980) are 470 μm and 568 μm for scales of photography of 1:10 000 and 1:50 000, respectively, which are twice the recommended size in this paper. Noukka *et al.* (1980) investigated the visibility of targets of different sizes and found that 100 μm circular targets at photograph scale were the most visible of those tested. These sizes are consistent with those given in this paper, though they have not been related to the optical magnification of observation. As shown earlier, optical magnification has a significant influence on optimum target size and the consequent pointing precisions.

The measuring precision for cross-type targets is marginally larger than that for circular targets. However, the difference between the precisions of the two target types is small for most applications; on the other hand, the effects of choosing cross-type targets of the wrong size are less severe than for circular targets. The main advantage of using the cross-type targets is that less material is required and, therefore, the cost of pre-flight targeting is reduced. A similar table to Table 1 can be deduced for a range of optical magnifications for cross-type targets if required.

## Conclusions

- An extensive series of pointing observations has been carried out on laboratory-prepared targets subject to blur and noise, and targets photographed during aerial photography. A universal figure has been derived from those observations, relating precision to the parameter of target size and characteristics of image quality, expressed as the slope of the density profile or spread function width and SNR. This diagram is sufficient to determine the pointing precision of any circular target for which the image quality characteristics are know.
- From these data, optimum target sizes and optical magnifications have been determined. These values should be suitable for most practical cases. Optical magnifications suitable for standard black-and-white aerial photography range from 12× to 24×. Pointing precisions obtainable under such circumstances range from 1.5 to 2 μm.
- Laboratory tests indicate that pointing precisions better than 1 μm can be achieved if the quality of the photography and optics of the stereoplotter are improved to that of a Gaussian point spread function with a 2σ-width of 10 μm or less. Such pointing precisions should be aimed for in practice.
- Studies of the aerial photography reveal that the laboratory observations have predicted results obtainable in practice with regard to optimum target size and pointing precisions.
- Measurements of image quality indicate a deterioration in image quality towards the edges of the format, and a better image quality when the red filter is used. However, such variations in image quality did not affect pointing precision, unless the targets were very small.
- Pointing precisions for color photography are superior to those for black-and-white photography, for the small circular targets. Indeed, the pointing precisions for small circular targets approach those obtainable with black-and-white photography with a Gaussian point spread function 2σ-width of 10 μm. Pointing precisions of about 1 μm should therefore be obtainable if color photography is used with current photographic systems, the observations being made at high optical magnification.
- Pointing precisions for cross-type targets are marginally lower than those for circular targets. For color photography there is an improvement in pointing precisions over those obtained with black-and-white photography.

## Acknowledgments

The research has been supported by a grant from the Australian Research Grants Scheme. The aerial photography has been obtained with the assistance of the Central Mapping Authority of N.S.W. (CMA). Target laying and survey of target positions were undertaken by officers of the CMA. Their contribution has been an important factor in the success of this project. The significant number of observations

were performed by the patient and willing students Ken Bullock, Paul Yeung and Elena Wong.

## References

Hufnagel, R. E., 1965. The Practical Application of Modulation Transfer Function. *Photographic Science and Engineering*, Vol. 9, pp. 235-264.

Noukka, P., A. Savolainen, and A. Laiho, 1980. An Empirical Study of the Visibility of Targets: *Proceedings ISPRS Congress Hamburg*, 1980, Vol. 23, No. B1, pp. 105-113.

O'Connor, D. C., 1967. *Visual Factors Affecting the Precision of Coordinate Measurements in Aerotriangulation*. University of Illinois, Photogrammetry Series No. 6.

Slama, C. C. (ed.), 1980. *Manual of Photogrammetry*, Fourth Edition, American Society of Photogrammetry, Falls Church, Va.

Snyder, H. L., M. E. Maddox, D. I. Shedivy, J. A. Turpin, J. J. Burke and R. N. Strickland, 1982. Digital Image Quality and Interpretability: Data Base and Hardcopy Studies. *Opitcal Engineering*, Vol. 21, pp. 14-22.

Trinder, J. C., 1971. Pointing Accuracies to Blurred Signals. *Photogrammetric Engineering*, Vol. 37, pp. 192-202.

———, 1973. Pointing Precision, Spread Function and MTF. *Photogrammetric Engineering*, Vol. 39, pp. 863-874.

———, 1974. *A Procedure for Selection of Ground Targets in Photogrammetry*. UNISURV G20, U.N.S.W., pp. 33-76.

———, 1980. Aerial Film Granularity and Its Influence on Visual Performance. *Proceedings International Society of Photogrammetry Congress*, Hamburg 1980, Vol. 23, No. B1, pp. 167-181.

———, 1982. Effects of Photographic Noise on Pointing Precision, Detection and Recognition. *Photogrammetric Engineering and Remote Sensing*, Vol. 48, pp. 1563-1575.

Welch, R., 1971. Modulation Transfer Functions. *Photogrammetric Engineering*, Vol. 37, pp. 247-259.

Ziemann, H., 1982. *Comparison of Camera Calibration Procedures:* Report prepared for German Research Foundation.

(Received 17 September 1983; accepted 22 March 1984; revised 15 May 1984)